



Le DAPNIA (Département d'Astrophysique, de physique des Particules, de physique Nucléaire et de l'Instrumentation Associée) regroupe les activités du Service d'Astrophysique (SAp), du Département de Physique des Particules Élémentaires (DPhPE) et du Département de Physique Nucléaire (DPhN).

Adresse : DAPNIA, Bâtiment 141  
CEA Saclay  
F - 91191 Gif-sur-Yvette Cedex

## On Sbottom hadronization at LEP 200.

Ph.Gris

CEA/DAPNIA/SPP Saclay

### Abstract

The question of the hadronization of the sbottom is of interest for experimental searches. A study concerning this feature is presented for masses accessible at LEP 200 assuming that the sbottom is the lightest squark. Numerical evaluations of the decay modes  $\tilde{b}_1 \rightarrow b\tilde{\chi}_1^0$  and  $\tilde{b}_1 \rightarrow b\tilde{\chi}_2^0$  are done by varying the SUSY space parameters  $M_2$  and  $\mu$ . The results obtained allow to assert in which conditions the sbottom hadronizes and which decay mode dominates.

# 1 Introduction

The supersymmetry (SUSY)[1] requires the existence of superpartners that differ from a spin 1/2 for all particles of the Standard Model. Hence the quark helicity states  $q_L$  and  $q_R$  have scalar partners  $\tilde{q}_L$  and  $\tilde{q}_R$ . Nonetheless, while  $\tilde{q}_L$  and  $\tilde{q}_R$  are supposed to be mass eigenstates (to a good approximation) for the two first generations, a strong mixing can appear for the third one, leading to a hard splitting between the mass eigenstates. It may even be possible that the lightest sbottom  $\tilde{b}_1$  is the lightest squark (especially for large values of  $\tan\beta$ , typically  $\tan\beta > 10$ .) [2].

The goal of this paper is to determine the dominant decay channels of the  $\tilde{b}_1$  considered as the lightest squark in the energy range of LEP 200 when  $R_{parity}$  is conserved. In particular, the channels  $\tilde{b}_1 \rightarrow b\tilde{\chi}_k^0$  are studied in detail, assuming that other decays are either kinematically forbidden (that is the case for  $\tilde{b}_1 \rightarrow t\tilde{\chi}_i^-$  or  $\tilde{b}_1 \rightarrow b\tilde{g}$ ) or negligible (an example is  $\tilde{b}_1 \rightarrow s\tilde{\chi}_k^0$  in which the flavour changing occur through loops). The computation of the decay width  $\Gamma(\tilde{b}_1 \rightarrow b\tilde{\chi}_k^0)$  allows to determine which decay dominates in which region of the SUSY space parameters and to assert whether the sbottom hadronizes or not. These two questions are of fundamental interest for the experimental search of the sbottom.

## 2 Theoretical framework

### 2.1 Sbottom mass matrix

The mass matrix of the sbottom in the  $(\tilde{b}_L, \tilde{b}_R)$  basis is given by [2]:

$$M_{\tilde{b}}^2 = \begin{pmatrix} m_{\tilde{b}_L}^2 & a_b m_b \\ a_b m_b & m_{\tilde{b}_R}^2 \end{pmatrix}$$

where

$$m_{\tilde{b}_L}^2 = M_{\tilde{Q}}^2 + m_b^2 - m_Z^2 \cos 2\beta \left( \frac{1}{2} - \frac{1}{3} \sin^2 \theta_W \right) \quad (1)$$

$$m_{\tilde{b}_R}^2 = M_{\tilde{D}}^2 + m_b^2 + \frac{1}{3} m_Z^2 \cos 2\beta \sin^2 \theta_W \quad (2)$$

$$a_b m_b = m_b (A_t - \mu \tan \beta) \quad (3)$$

The parameters involved are the Higgs mass superfield  $\mu$ , the ratio of the two Higgs vacuum expectation values  $\tan\beta$ , the soft-supersymmetry breaking terms  $M_{\tilde{Q}}^2$  and  $M_{\tilde{D}}^2$ , the Higgs-squark-squark trilinear interaction term proportionnal to  $A_t$ .

The mass eigenstates  $\tilde{b}_1$  and  $\tilde{b}_2$  (with  $m_{\tilde{b}_1} < m_{\tilde{b}_2}$ ) are related to  $\tilde{b}_L$  and  $\tilde{b}_R$  through the relations :

$$\tilde{b}_1 = \cos\theta_{\tilde{b}} \tilde{b}_L + \sin\theta_{\tilde{b}} \tilde{b}_R \quad (4)$$

$$\tilde{b}_2 = -\sin\theta_{\tilde{b}} \tilde{b}_L + \cos\theta_{\tilde{b}} \tilde{b}_R \quad (5)$$

The mixing angle  $\theta_{\tilde{b}}$  is given by:

$$\cos\theta_{\tilde{b}} = -a_b m_b \sqrt{\frac{1}{(m_{\tilde{b}_L}^2 - m_{\tilde{b}_R}^2)^2 + 4a_b^2 m_b^2}}, \quad \sin\theta_{\tilde{b}} = \sqrt{\frac{(m_{\tilde{b}_L}^2 - m_{\tilde{b}_R}^2)^2}{(m_{\tilde{b}_L}^2 - m_{\tilde{b}_R}^2)^2 + 4a_b^2 m_b^2}} \quad (6)$$

and their masses are given by :

$$m_{\tilde{b}_{1,2}}^2 = \frac{1}{2}[m_{\tilde{b}_L}^2 + m_{\tilde{b}_R}^2 \mp \sqrt{(m_{\tilde{b}_L}^2 - m_{\tilde{b}_R}^2)^2 + 4a_b^2 m_b^2}] \quad (7)$$

As it can be seen from (6) and (7),  $a_b m_b$  (and thus  $\tan\beta$  through (3)) rules the splitting and the mixing between the two mass eigenstates.

## 2.2 Decay formulae

The sbottom interaction with neutralinos is deduced from [2]:

$$\mathcal{L} = g\bar{f}(a_{ik}^b P_L + b_{ik}^b P_R)\tilde{\chi}_k^0 \tilde{b}_i + hc \quad (8)$$

with

$$\begin{pmatrix} a_{1k}^b \\ a_{2k}^b \end{pmatrix} = \begin{pmatrix} \cos\theta_{\tilde{b}} & \sin\theta_{\tilde{b}} \\ -\sin\theta_{\tilde{b}} & \cos\theta_{\tilde{b}} \end{pmatrix} \begin{pmatrix} h_{Lk}^b \\ f_{Rk}^b \end{pmatrix}, \quad \begin{pmatrix} b_{1k}^b \\ b_{2k}^b \end{pmatrix} = \begin{pmatrix} \cos\theta_{\tilde{b}} & \sin\theta_{\tilde{b}} \\ -\sin\theta_{\tilde{b}} & \cos\theta_{\tilde{b}} \end{pmatrix} \begin{pmatrix} f_{Lk}^b \\ h_{Rk}^b \end{pmatrix}$$

and

$$h_{Lk}^b = h_{Rk}^b = -Y_b(N_{k3}\cos\beta + N_{k4}\sin\beta) \quad (9)$$

$$f_{Lk}^b = \frac{\sqrt{2}}{3}\sin\theta_W N_{k1} + \sqrt{2}\left(\frac{1}{2} - \frac{1}{3}\sin^2\theta_W\right)\frac{N_{k2}}{\cos\theta_W} \quad (10)$$

$$f_{Rk}^b = \frac{\sqrt{2}}{3}\sin\theta_W(\tan\theta_W N_{k2} - N_{k1}) \quad (11)$$

$Y_b$  is the Yukawa coupling :

$$Y_b = \frac{m_b}{(\sqrt{2}m_W \cos\beta)} \quad (12)$$

$N_{ij}$  is the 4x4 unitary matrix diagonalizing the neutral gaugino-higgsino mass matrix  $M_{\tilde{\chi}_k^0}$ . In the basis  $(\tilde{\gamma}, \tilde{Z}^0, \tilde{H}_a^0, \tilde{H}_b^0)$  (with  $\tilde{\gamma} = \cos\theta_W \tilde{B} + \sin\theta_W \tilde{W}_3$ ,  $\tilde{Z}^0 = -\sin\theta_W \tilde{B} + \cos\theta_W \tilde{W}_3$ ,  $\tilde{H}_a^0 = \tilde{H}_1^0 \cos\beta - \tilde{H}_2^0 \sin\beta$ ,  $\tilde{H}_b^0 = \tilde{H}_1^0 \sin\beta + \tilde{H}_2^0 \cos\beta$ ),  $M_{\tilde{\chi}_k^0}$  is given by :

$$M_{\tilde{\chi}_k^0} = \begin{pmatrix} M_2 \sin^2\theta_W + M_1 \cos^2\theta_W & (M_2 - M_1) \cos\theta_W \sin\theta_W & 0 & 0 \\ (M_2 - M_1) \cos\theta_W \sin\theta_W & M_2 \cos^2\theta_W + M_1 \sin^2\theta_W & M_z & 0 \\ 0 & M_z & \mu \sin 2\beta & -\mu \cos 2\beta \\ 0 & 0 & -\mu \cos 2\beta & -\mu \sin 2\beta \end{pmatrix}$$

At the tree level, the decay width of the interaction  $\tilde{b}_i \rightarrow b\tilde{\chi}_k^0$  is given by:

$$\Gamma(\tilde{b}_i \rightarrow b\tilde{\chi}_k^0) = \frac{g^2 \lambda^{\frac{1}{2}}(m_{\tilde{b}_i}^2, m_b^2, m_{\tilde{\chi}_k^0}^2)}{16\pi m_{\tilde{b}_i}^3} [(a_{ik}^2 + b_{ik}^2)(m_{\tilde{b}_i}^2 - m_b^2 - m_{\tilde{\chi}_k^0}^2) - 4a_{ik}b_{ik}m_b m_{\tilde{\chi}_k^0}^2] \quad (13)$$

where  $\lambda(x, y, z) = x^2 + y^2 + z^2 - 2xy - 2xz - 2yz$ .

For the following, only the lightest sbottom  $\tilde{b}_1$  is treated. Moreover, the GUT relation  $M_1 = \frac{5}{3}M_2 \tan^2 \theta_W$  is assumed. The parameters that rule  $\Gamma(\tilde{b}_i \rightarrow b\tilde{\chi}_k^0)$  are thus  $m_{\tilde{b}_i}, \theta_{\tilde{b}_i}, \mu, M_2$  and  $\tan \beta$ .

### 3 $\tilde{b}_1$ hadronization and $\tilde{\chi}_k^0$ composition: numerical results

The matrix  $M_{\tilde{\chi}_k^0}$  indicates that the mass eigenstates are highly dependant on the SUSY parameters. More precisely, the composition of  $\tilde{\chi}_1^0, \tilde{\chi}_2^0, \tilde{\chi}_3^0, \tilde{\chi}_4^0$  in photino, zino and higgsino are ruled by the relatives values of  $M_2$  and  $\mu$  (the dependance on  $\tan \beta$  is quite small). Three domains depending on  $(M_2, \mu)$  can be distinguished:

- $|\mu| \gg M_2$  :  $\tilde{\chi}_1^0, \tilde{\chi}_2^0$  are jaugino-like,  $\tilde{\chi}_3^0, \tilde{\chi}_4^0$  are higgsino-like.
- $M_2 \sim |\mu|$  :  $\tilde{\chi}_1^0, \tilde{\chi}_2^0, \tilde{\chi}_3^0, \tilde{\chi}_4^0$  are a mixing of jaugino and higgsino.
- $M_2 \gg |\mu|$  :  $\tilde{\chi}_1^0, \tilde{\chi}_2^0$  are higgsino-like,  $\tilde{\chi}_3^0, \tilde{\chi}_4^0$  are jaugino-like.

A numerical evaluation of  $M_{\tilde{\chi}_1^0}, M_{\tilde{\chi}_2^0}, M_{\tilde{\chi}_3^0}, M_{\tilde{\chi}_4^0}$ , as well as the compositions in jaugino/higgsino, has been done. It was then assumed that the only possible decays of  $\tilde{b}_1$  were:  $\tilde{b}_1 \rightarrow b\tilde{\chi}_1^0$  and  $\tilde{b}_1 \rightarrow b\tilde{\chi}_2^0$ .

The decay widths of each mode has been computed to determine in which cases the sbottom hadronizes: as the typical QCD time-scale is about  $10^{-23}$  s, we get  $\Gamma_{QCD} \sim 0.06$  Gev. If the widths of  $\tilde{b}_1$  are lower than  $\Gamma_{QCD}$ ,  $\tilde{b}_1$  hadronizes first before decaying. Furthermore, the branching ratio of  $\tilde{b}_1 \rightarrow b\tilde{\chi}_1^0$  has been computed to evaluate whether this decay dominates or not. Two values of  $\tan \beta$  (bigger than 10 because of the assumption that  $\tilde{b}_1$  is the lightest squark [2]) were used for the numerical calculations:  $\tan \beta = 15$ . and  $\tan \beta = 35$ .

#### 3.1 $|\mu| \gg M_2$

In this case,  $M_2$  has been taken equal to 50 and  $\mu$  to 450 (the conclusions are the same for  $\mu < 0$ ). The two first neutralinos are then jaugino-like as it can be seen in table 1.

What can immediatly be seen in fig.1 is that the width of both  $\tilde{b}_1 \rightarrow b\tilde{\chi}_1^0$  and  $\tilde{b}_1 \rightarrow b\tilde{\chi}_2^0$  are strongly dependant on the mixing angle  $\theta_{\tilde{b}_i}$ . An increase of the widths is observed with the rise of  $\tan \beta$ . Moreover, a sbottom right does not seem to hadronize (it is quite difficult to conclude because the width is not really higher from  $\Gamma_{QCD}$ ) in the decay  $\tilde{b}_1 \rightarrow b\tilde{\chi}_1^0$  whereas it does in  $\tilde{b}_1 \rightarrow b\tilde{\chi}_2^0$ . The conclusions are inversed for a sbottom left.

This great dependance of the width on the mixing angle can be explain by the sbottom-bottom-zino coupling. As it can be deduced from eqs (10) and (11), the coupling of  $\tilde{b}_1$  to the photino does not depend on  $\theta_{\tilde{b}_i}$  whereas it does for the zino: in fact, the  $\tilde{b}_1$ -b- $\tilde{Z}^0$  interaction favours  $\tilde{b}_L$ .  $\Gamma(\tilde{b}_1 \rightarrow b\tilde{\chi}_2^0)$  is thus quite small for a sbottom right because  $\tilde{\chi}_2^0$  is rather zino (table 1). The difference between  $\tilde{b}_L$  and  $\tilde{b}_R$  is not obvious for  $\Gamma(\tilde{b}_1 \rightarrow$

$b\tilde{\chi}_1^0$ ) on account of the photino dominance of  $\tilde{\chi}_1^0$  ( $\tilde{b}_R$  is here favoured thanks to a negative contribution of the zino part - see table 1).

An other effect of the high-dependance on the mixing angle of the zino coupling is the variations of the branching ratio of  $\tilde{b}_1 \rightarrow b\tilde{\chi}_1^0$  (see fig.1)

### 3.2 $M_2 \sim |\mu|$

In order to estimate the sensibility of the results to the parameters  $M_2$  and  $\mu$ , few couples of values of  $(M_2, \mu)$  have been used(see tables 2,3,4).

What can immediatly be seen in fig.2,3 and 4 is that  $\tilde{b}_1$  does not hadronize in the decay  $\tilde{b}_1 \rightarrow b\tilde{\chi}_1^0$ . This is due to the fact that when  $M_2 \sim |\mu|$ ,  $\tilde{\chi}_1^0$  is a mixing of higgsino and jaugino (roughly we have 30%  $\tilde{\gamma}$ , 30%  $\tilde{Z}^0$ , 30%  $\tilde{H}_b^0$ ) and the problem due to the zino coupling (ie the dependance on  $\theta_{\tilde{b}}$  see section 3.1) does not appear, both because the zino contribution is negative and because the photino and higgsino contributions (which are independant of  $\theta_{\tilde{b}}$ ) are high enough.

In the decay  $\tilde{b}_1 \rightarrow b\tilde{\chi}_2^0$ , one has again to consider the cases of a sbottom left and of a right. This is due to the fact that even if  $\tilde{\chi}_2^0$  is rather photino, a positive contribution of the zino tends to reduce the width of  $\tilde{b}_1 \rightarrow b\tilde{\chi}_2^0$  for a sbottom right (as it is visible for instance on fig.4). The sbottom does not hadronize however.

The branching of  $\tilde{b}_1 \rightarrow b\tilde{\chi}_1^0$  is rather independant on the mixing angle and show a clear domination of this decay over  $\tilde{b}_1 \rightarrow b\tilde{\chi}_2^0$ . The small accident visible on fig.4 is due to the choice of the SUSY parameters and disappear with the increase of  $\tan\beta$ .

### 3.3 $M_2 \gg |\mu|$

In that case,  $\tilde{\chi}_1^0$  and  $\tilde{\chi}_2^0$  are higgsino-like(table 5). As the coupling sbottom-bottom-higgsino does not depend on the mixing angle  $\theta_{\tilde{b}}$  (see (9)), a high width in the two modes  $\tilde{b}_1 \rightarrow b\tilde{\chi}_1^0$  and  $\tilde{b}_1 \rightarrow b\tilde{\chi}_2^0$  is obtained. The sbottom does not hadronize in that case (fig.5) and the decay in  $b\tilde{\chi}_1^0$  dominates for all mixing angle.

## 4 Conclusions

The numerical results concerning the widths of  $\tilde{b}_1 \rightarrow b\tilde{\chi}_1^0$  and  $\tilde{b}_1 \rightarrow b\tilde{\chi}_2^0$  gave the following results:

- $|\mu| \gg M_2$  :  $\tilde{\chi}_1^0$  and  $\tilde{\chi}_2^0$  are jaugino like. The fact that the sbottom hadronizes or not and the dominant decay mode (between  $b\tilde{\chi}_1^0$  and  $b\tilde{\chi}_2^0$ ) strongly depend on the mixing angle  $\theta_{\tilde{b}}$ .
- $M_2 \sim |\mu|$  :  $\tilde{\chi}_1^0$  and  $\tilde{\chi}_2^0$  are a mixing of jaugino and higgsino. Except for some values of the mixing angle depending on the choice of the SUSY parameters, the sbottom does not hadronize and the decay  $\tilde{b}_1 \rightarrow b\tilde{\chi}_1^0$  dominates.
- $M_2 \gg |\mu|$  :  $\tilde{\chi}_1^0$  and  $\tilde{\chi}_2^0$  are higgsino-like. The sbottom does not hadronize and  $\tilde{b}_1 \rightarrow b\tilde{\chi}_1^0$  dominates for all  $\theta_{\tilde{b}}$

Important experimental consequences can be deduced from that. If  $\tilde{b}_1 \rightarrow b\tilde{\chi}_1^0$  dominates, the signature of the signal is quite simple: a b-jet+missing  $p_t$ . It is quite different when  $\tilde{b}_1 \rightarrow b\tilde{\chi}_2^0$  is preeminent, because of the decay of  $\tilde{\chi}_2^0$ : a manifestation of  $\tilde{b}_1$  would then be either 3 jets (with one b)+missing  $p_t$  or one b-jet+lepton+missing  $p_t$ .

## Acknowledgements

I thank V.Ruhmann-Kleider and M.Besançon for encouraging this work. I am grateful to M.Besançon for the reading of the manuscript.

## References

- [1] H.P.Nilles,Phys.Rep. 110(1984) 1  
H.E.Haber,G.L.Kane,Phys.Rep. 117(1985) 75
- [2] A.Bartl,W.Majerotto,W.Porod Z.Phys.C 64(1994) 499

## FIGURE CAPTIONS

- Figure 1 : Decay widths of the sbottom for two values of  $\tan\beta$ (15 and 35) for a sbottom right(dashed line) and a sbottom left(solid line) for  $M_2 = 50, \mu = 450$ . The branching ratio of  $\tilde{b}_1 \rightarrow b\tilde{\chi}_1^0$  as a function of  $\theta_{\tilde{b}}$  is drawn for three masses of  $\tilde{b}_1$  :  $m_{\tilde{b}_1} = 55$  Gev(so,solid line),  $m_{\tilde{b}_1} = 90$  Gev(dotted line) and  $m_{\tilde{b}_1} = 100$  Gev(dashed line)
- Figure 2 : Decay widths of the sbottom for two values of  $\tan\beta$ (15 and 35) for a sbottom right(dashed line) and a sbottom left(solid line) for  $M_2 = 100, \mu = 80$ . The branching ratio of  $\tilde{b}_1 \rightarrow b\tilde{\chi}_1^0$  as a function of  $\theta_{\tilde{b}}$  is drawn for three masses of  $\tilde{b}_1$  :  $m_{\tilde{b}_1} = 80$  Gev(so,solid line),  $m_{\tilde{b}_1} = 100$  Gev(dotted line) and  $m_{\tilde{b}_1} = 120$  Gev(dashed line)
- Figure 3 : Decay widths of the sbottom for two values of  $\tan\beta$ (15 and 35) for a sbottom right(dashed line) and a sbottom left(solid line) for  $M_2 = 80, \mu = 100$ . The branching ratio of  $\tilde{b}_1 \rightarrow b\tilde{\chi}_1^0$  as a function of  $\theta_{\tilde{b}}$  is drawn for three masses of  $\tilde{b}_1$  :  $m_{\tilde{b}_1} = 90$  Gev(so,solid line),  $m_{\tilde{b}_1} = 90$  Gev(dotted line) and  $m_{\tilde{b}_1} = 100$  Gev(dashed line)
- Figure 4 : Decay widths of the sbottom for two values of  $\tan\beta$ (15 and 35) for a sbottom right(dashed line) and a sbottom left(solid line) for  $M_2 = 80, \mu = -100$ . The branching ratio of  $\tilde{b}_1 \rightarrow b\tilde{\chi}_1^0$  as a function of  $\theta_{\tilde{b}}$  is drawn for three masses of  $\tilde{b}_1$  :  $m_{\tilde{b}_1} = 90$  Gev(so,solid line),  $m_{\tilde{b}_1} = 90$  Gev(dotted line) and  $m_{\tilde{b}_1} = 100$  Gev(dashed line)
- Figure 5 : Decay widths of the sbottom for two values of  $\tan\beta$ (15 and 35) for a sbottom right(dashed line) and a sbottom left(solid line) for  $M_2 = 500, \mu = 50$ . The branching ratio of  $\tilde{b}_1 \rightarrow b\tilde{\chi}_1^0$  as a function of  $\theta_{\tilde{b}}$  is drawn for three masses of  $\tilde{b}_1$  :  $m_{\tilde{b}_1} = 65$  Gev(so,solid line),  $m_{\tilde{b}_1} = 90$  Gev(dotted line) and  $m_{\tilde{b}_1} = 120$  Gev(dashed line)

$\tan \beta = 15.$	Mass(Gev)	% $\tilde{\gamma}$	% $Z^0$	% $H_a^0$	% $H_b^0$	Physical state
$\tilde{\chi}_1^0$	24.2	70.49	28.32	0.04	1.15	$.84\tilde{\gamma} - .53Z^0 + .02H_a^0 + .11H_b^0$
$\tilde{\chi}_2^0$	46.8	29.51	67.55	0.16	2.78	$.54\tilde{\gamma} + .82Z^0 - .04H_a^0 - .17H_b^0$
$\tilde{\chi}_3^0$	457.3	0.00	2.72	55.77	41.51	$.00\tilde{\gamma} - .16Z^0 + .75H_a^0 + .64H_b^0$
$\tilde{\chi}_4^0$	461.4	0.00	2.69	56.17	41.14	$.00\tilde{\gamma} + .16Z^0 + .75H_a^0 + .64H_b^0$
$\tan \beta = 35.$	Mass(Gev)	% $\tilde{\gamma}$	% $Z^0$	% $H_a^0$	% $H_b^0$	Physical state
$\tilde{\chi}_1^0$	24.6	72.89	26.03	0.01	1.07	$.85\tilde{\gamma} - .51Z^0 + .01H_a^0 + .10H_b^0$
$\tilde{\chi}_2^0$	47.7	27.11	69.89	0.08	2.93	$.52\tilde{\gamma} + .84Z^0 - .03H_a^0 - .17H_b^0$
$\tilde{\chi}_3^0$	457.9	0.00	2.55	52.31	45.15	$.00\tilde{\gamma} - .16Z^0 + .72H_a^0 + .67H_b^0$
$\tilde{\chi}_4^0$	460.7	0.00	2.52	52.60	44.88	$.00\tilde{\gamma} - .16Z^0 + .73H_a^0 + .67H_b^0$

Table 1:  $M_2 = 50, \mu = 450$

$\tan \beta = 15.$	Mass(Gev)	% $\tilde{\gamma}$	% $Z^0$	% $H_a^0$	% $H_b^0$	Physical state
$\tilde{\chi}_1^0$	25.1	10.20	31.11	9.88	48.81	$.32\tilde{\gamma} - .56Z^0 + .31H_a^0 + .70H_b^0$
$\tilde{\chi}_2^0$	63.6	87.22	0.68	5.65	6.45	$.93\tilde{\gamma} + .08Z^0 - .24H_a^0 - .25H_b^0$
$\tilde{\chi}_3^0$	102.2	21.17	78.71	0.08	0.04	$-.46\tilde{\gamma} - .89Z^0 + .03H_a^0 + .02H_b^0$
$\tilde{\chi}_4^0$	163.8	2.39	56.38	34.17	7.06	$.15\tilde{\gamma} + .75Z^0 + .58H_a^0 + .27H_b^0$
$\tan \beta = 35.$	Mass(Gev)	% $\tilde{\gamma}$	% $Z^0$	% $H_a^0$	% $H_b^0$	Physical state
$\tilde{\chi}_1^0$	27.8	11.47	30.03	8.23	50.26	$.34\tilde{\gamma} - .55Z^0 + .29H_a^0 + .71H_b^0$
$\tilde{\chi}_2^0$	63.8	85.85	0.79	5.64	7.71	$.93\tilde{\gamma} + .09Z^0 - .24H_a^0 - .28H_b^0$
$\tilde{\chi}_3^0$	103.7	19.98	79.69	0.21	0.11	$-.45\tilde{\gamma} - .89Z^0 + .05H_a^0 + .03H_b^0$
$\tilde{\chi}_4^0$	162.4	2.48	56.89	33.07	7.57	$.16\tilde{\gamma} + .75Z^0 + .58H_a^0 + .28H_b^0$

Table 2:  $M_2 = 100, \mu = 80$

$\tan \beta = 15.$	Mass(Gev)	% $\tilde{\gamma}$	% $\tilde{Z}^0$	% $\tilde{H}_a^0$	% $\tilde{H}_b^0$	Physical state
$\tilde{\chi}_1^0$	25.1	18.78	39.24	5.47	36.51	$.43\tilde{\gamma} - .63\tilde{Z}^0 + .23\tilde{H}_a^0 + .60\tilde{H}_b^0$
$\tilde{\chi}_2^0$	53.9	80.14	5.89	4.40	9.57	$.90\tilde{\gamma} + .24\tilde{Z}^0 - .21\tilde{H}_a^0 - .31\tilde{H}_b^0$
$\tilde{\chi}_3^0$	121.3	3.74	68.61	17.93	9.72	$-.19\tilde{\gamma} - .83\tilde{Z}^0 + .42\tilde{H}_a^0 + .31\tilde{H}_b^0$
$\tilde{\chi}_4^0$	162.4	0.97	43.81	41.89	13.33	$.10\tilde{\gamma} + .66\tilde{Z}^0 + .65\tilde{H}_a^0 + .37\tilde{H}_b^0$
$\tan \beta = 35.$	Mass(Gev)	% $\tilde{\gamma}$	% $\tilde{Z}^0$	% $\tilde{H}_a^0$	% $\tilde{H}_b^0$	Physical state
$\tilde{\chi}_1^0$	27.7	22.37	37.30	4.06	36.27	$.47\tilde{\gamma} - .61\tilde{Z}^0 + .20\tilde{H}_a^0 + .60\tilde{H}_b^0$
$\tilde{\chi}_2^0$	54.5	76.52	7.14	4.36	11.98	$.87\tilde{\gamma} + .27\tilde{Z}^0 - .21\tilde{H}_a^0 - .35\tilde{H}_b^0$
$\tilde{\chi}_3^0$	122.8	3.50	66.69	18.59	11.22	$-.19\tilde{\gamma} - .82\tilde{Z}^0 + .43\tilde{H}_a^0 + .34\tilde{H}_b^0$
$\tilde{\chi}_4^0$	160.7	1.00	44.01	40.44	14.55	$.10\tilde{\gamma} + .66\tilde{Z}^0 + .64\tilde{H}_a^0 + .38\tilde{H}_b^0$

Table 3:  $M_2 = 80, \mu = 100$

$\tan \beta = 15.$	Mass(Gev)	% $\tilde{\gamma}$	% $\tilde{Z}^0$	% $\tilde{H}_a^0$	% $\tilde{H}_b^0$	Physical state
$\tilde{\chi}_1^0$	33.7	35.44	30.99	1.36	32.20	$.60\tilde{\gamma} - .56\tilde{Z}^0 - .56\tilde{H}_a^0 - .57\tilde{H}_b^0$
$\tilde{\chi}_2^0$	56.6	63.34	11.79	4.00	20.88	$.80\tilde{\gamma} + .34\tilde{Z}^0 + .34\tilde{H}_a^0 + .46\tilde{H}_b^0$
$\tilde{\chi}_3^0$	126.2	2.95	61.78	19.93	15.34	$-.17\tilde{\gamma} - .79\tilde{Z}^0 + .45\tilde{H}_a^0 - .39\tilde{H}_b^0$
$\tilde{\chi}_4^0$	156.1	1.11	44.59	36.65	17.65	$.11\tilde{\gamma} + .67\tilde{Z}^0 + .61\tilde{H}_a^0 - .42\tilde{H}_b^0$
$\tan \beta = 35.$	Mass(Gev)	% $\tilde{\gamma}$	% $\tilde{Z}^0$	% $\tilde{H}_a^0$	% $\tilde{H}_b^0$	Physical state
$\tilde{\chi}_1^0$	31.4	29.47	33.79	2.28	34.46	$.54\tilde{\gamma} - .58\tilde{Z}^0 + .15\tilde{H}_a^0 - .59\tilde{H}_b^0$
$\tilde{\chi}_2^0$	55.7	69.36	9.65	4.20	16.79	$.83\tilde{\gamma} + .31\tilde{Z}^0 - .20\tilde{H}_a^0 + .41\tilde{H}_b^0$
$\tilde{\chi}_3^0$	124.9	3.16	63.75	19.45	13.65	$-.18\tilde{\gamma} - .80\tilde{Z}^0 + .44\tilde{H}_a^0 - .37\tilde{H}_b^0$
$\tilde{\chi}_4^0$	158.0	1.06	44.34	38.19	16.41	$.10\tilde{\gamma} + .67\tilde{Z}^0 + .62\tilde{H}_a^0 - .41\tilde{H}_b^0$

Table 4:  $M_2 = 80, \mu = -100$

$\tan \beta = 15.$	Mass(Gev)	% $\tilde{\gamma}$	% $\tilde{Z}^0$	% $\tilde{H}_a^0$	% $\tilde{H}_b^0$	Physical state
$\tilde{\chi}_1^0$	38.3	0.42	2.76	43.74	53.09	$.06\tilde{\gamma} - .17\tilde{Z}^0 - .66\tilde{H}_a^0 + .73\tilde{H}_b^0$
$\tilde{\chi}_2^0$	58.4	0.76	4.32	60.07	34.84	$-.09\tilde{\gamma} + .21\tilde{Z}^0 + .78\tilde{H}_a^0 + .59\tilde{H}_b^0$
$\tilde{\chi}_3^0$	258.2	79.06	18.26	2.59	0.09	$.89\tilde{\gamma} - .43\tilde{Z}^0 - .16\tilde{H}_a^0 - .03\tilde{H}_b^0$
$\tilde{\chi}_4^0$	512.9	20.37	77.06	2.55	0.02	$.45\tilde{\gamma} + .88\tilde{Z}^0 + .16\tilde{H}_a^0 + .02\tilde{H}_b^0$
$\tan \beta = 35.$	Mass(Gev)	% $\tilde{\gamma}$	% $\tilde{Z}^0$	% $\tilde{H}_a^0$	% $\tilde{H}_b^0$	Physical state
$\tilde{\chi}_1^0$	39.2	0.39	2.55	40.27	56.79	$.06\tilde{\gamma} - .16\tilde{Z}^0 + .63\tilde{H}_a^0 + .75\tilde{H}_b^0$
$\tilde{\chi}_2^0$	59.1	0.74	4.17	57.65	37.44	$-.09\tilde{\gamma} + .20\tilde{Z}^0 + .76\tilde{H}_a^0 + .61\tilde{H}_b^0$
$\tilde{\chi}_3^0$	258.1	79.06	18.33	2.52	0.09	$.89\tilde{\gamma} - .43\tilde{Z}^0 - .16\tilde{H}_a^0 - .03\tilde{H}_b^0$
$\tilde{\chi}_4^0$	512.8	20.39	77.07	2.51	0.02	$.45\tilde{\gamma} + .88\tilde{Z}^0 + .16\tilde{H}_a^0 + .02\tilde{H}_b^0$

Table 5:  $M_2 = 500, \mu = 50$

$M_2=50, \mu=450$  (neutralinos jaugino-like)  
 $\tan\beta=15.$   $\tan\beta=35.$

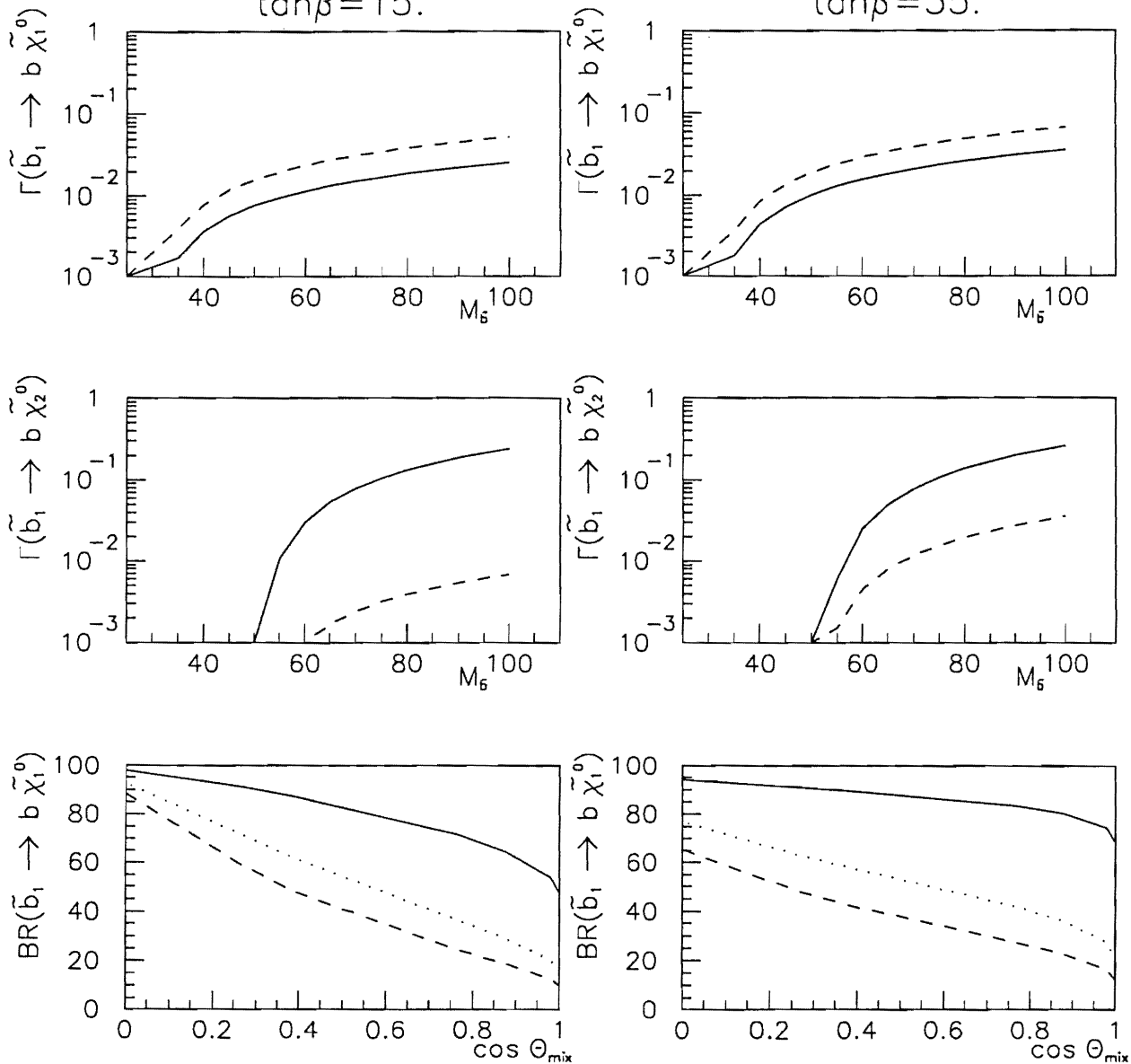


fig. 1

$M_2=100, \mu=80$  (neutralinos jaugino/higgsino)

$\tan\beta=15.$

$\tan\beta=35.$

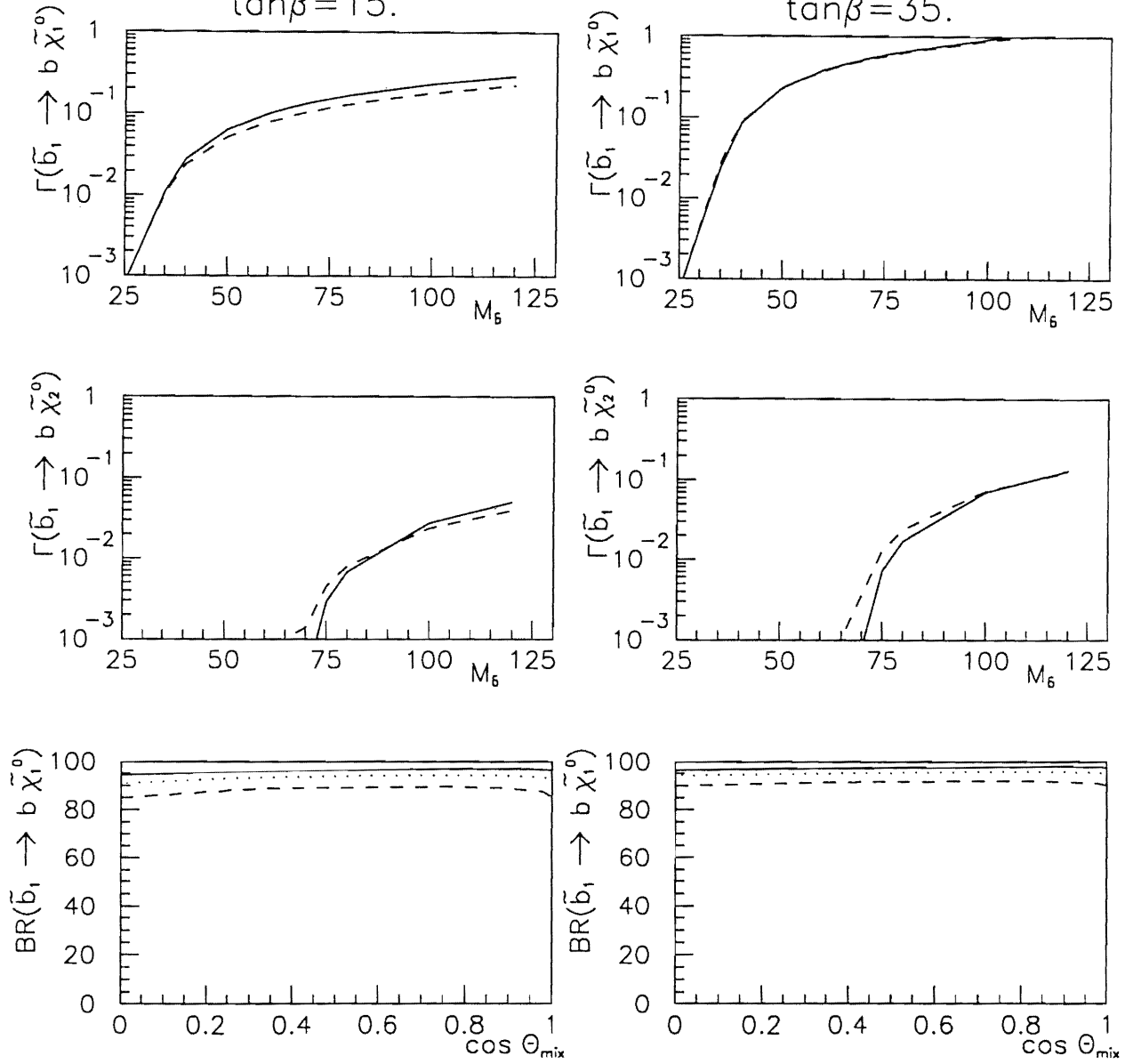


fig. 2

$M_2=80, \mu=100$  (neutralinos jaugino/higgsino)  
 $\tan\beta=15.$   $\tan\beta=35.$

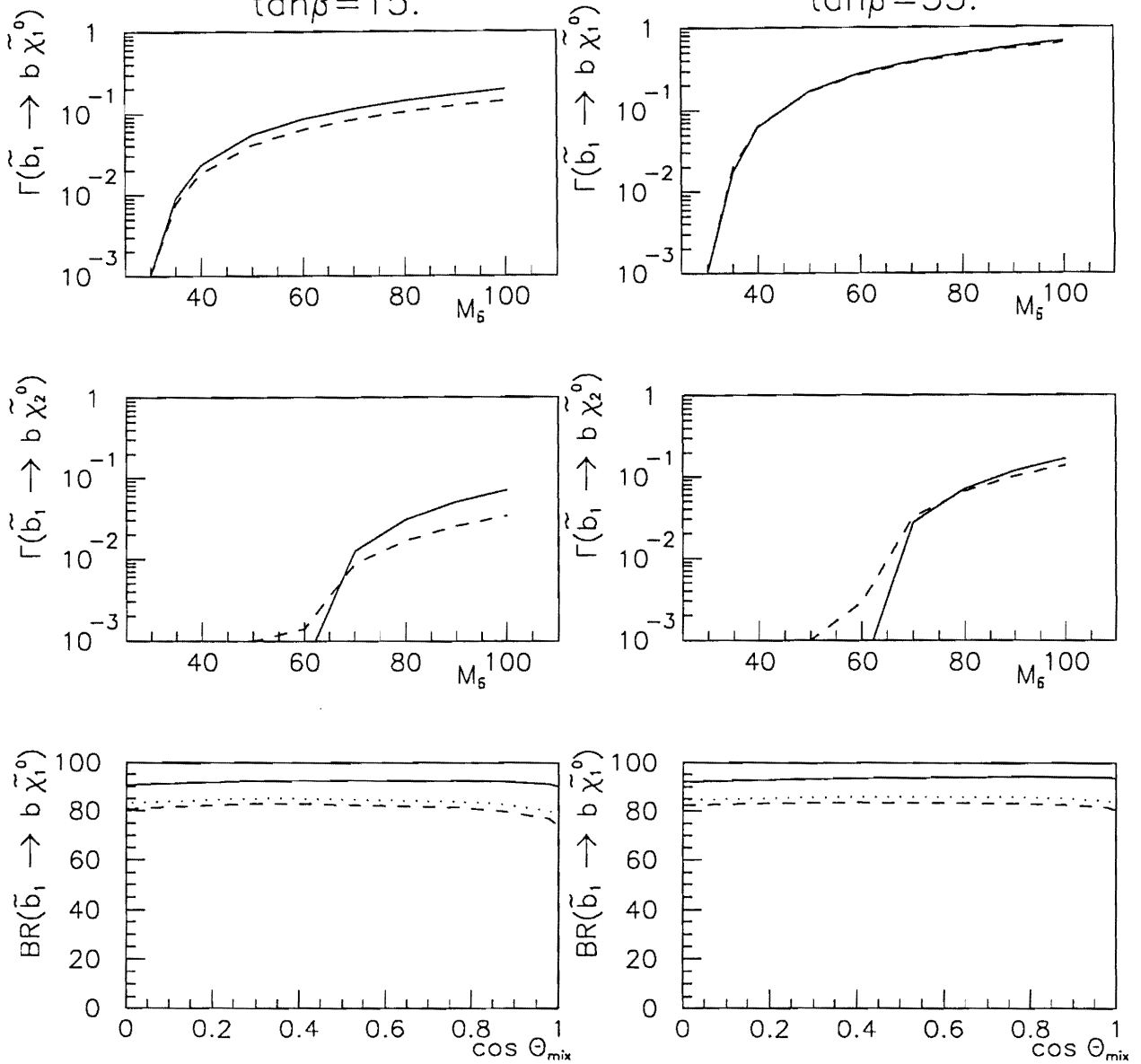


fig. 3

$M_2=80, \mu=-100$  (neutralinos jaugino/higgsino)

$\tan\beta=15.$

$\tan\beta=35.$

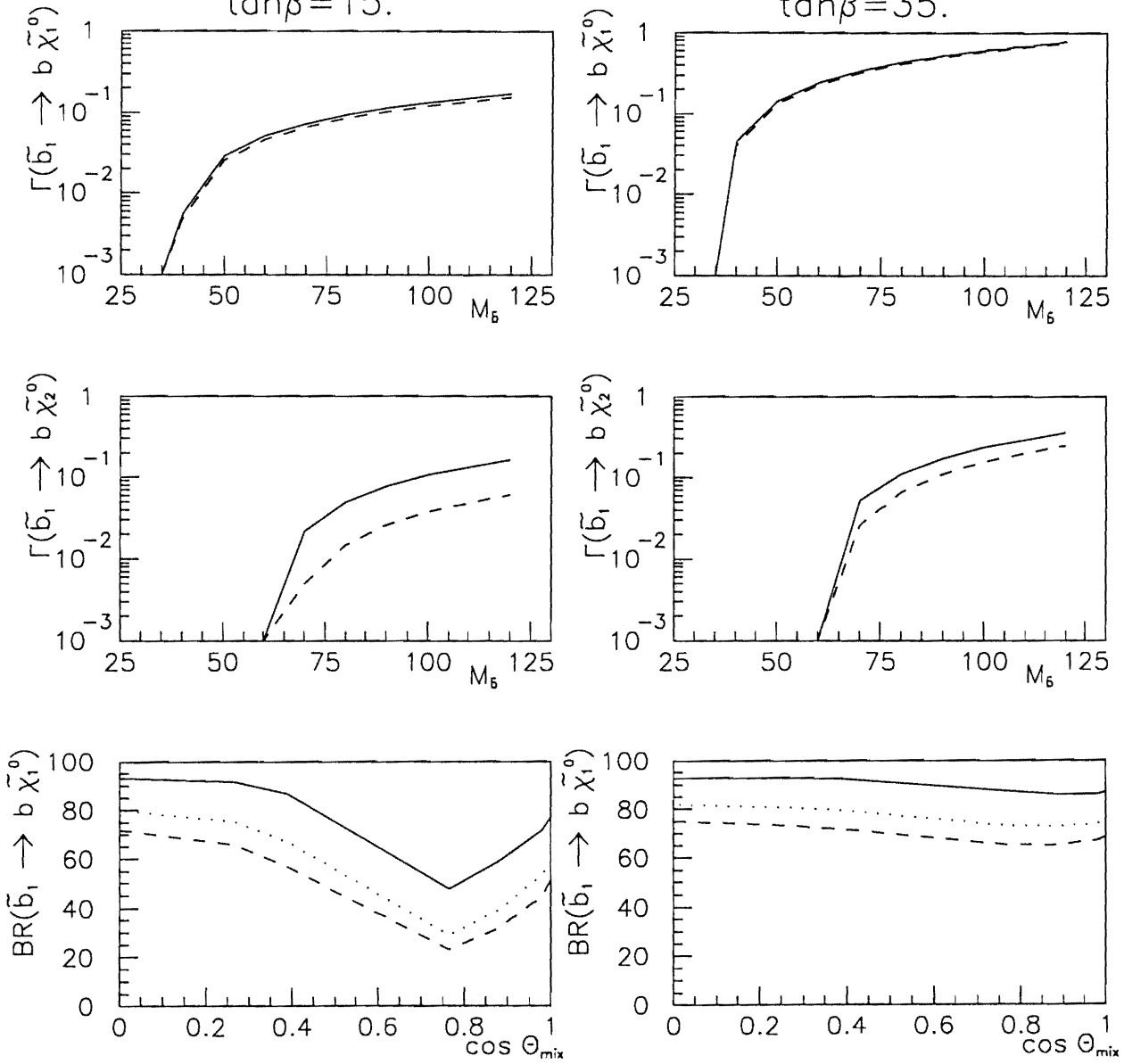


fig. 4

$M_2=500, \mu=50$  (neutralinos higgsino-like)

$\tan\beta=15.$

$\tan\beta=35.$

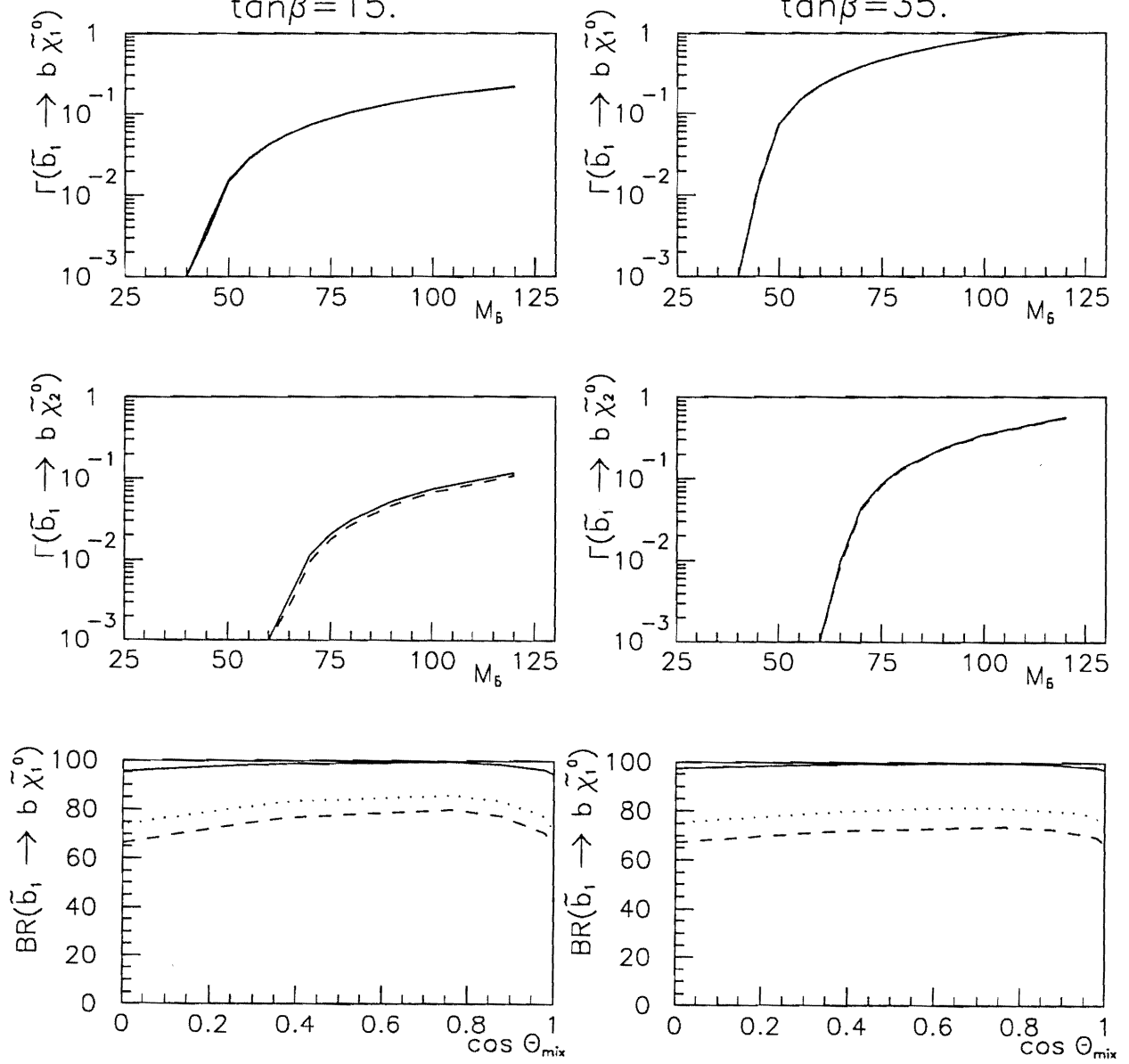


fig. 5